Main criteria of sustainable natural fibre for efficient unidirectional biocomposites

Alain Bourmaud, Justin Merotte, David Siniscalco, Maelenn Le Gall, Victor Gager, Antoine Le Duigou, Floran Pierre, Karim Behlouli, Olivier Arnould, Johnny Beaugrand, et al.

Main criteria of sustainable natural fibre for efficient unidirectional biocomposites

Alain Bourmaud[a,*], Justin Mérotte[a], David Siniscalco[a], Maelenn Le Gall[b], Victor Gager[a,c], Antoine Le Duigou[a], Floran Pierre[c], Karim Behlouli[c], Olivier Arnould[d], Johnny Beaugrand[e,f], Christophe Baley[a]

[a] Univ. Bretagne Sud, UMR CNRS 6027, IRDL, 56100 Lorient, France
[b] IFREMER Centre Bretagne, Marine Structures Laboratory, 29280 Plouzané, France
[c] EcoTechnilin SAS, ZA Caux Multipôles, 76190 Valliquerville, France
[d] LMGC, Université de Montpellier, CNRS, UMR 5508, Montpellier, France
[e] UMR FARE, INRA, Université de Reims Champagne-Ardenne, 2 Esplanade Roland-Garros, 51100 Reims, France
[f] UR1268 Biopolymères Interactions Assemblages, INRA, 44316 Nantes, France

A B S T R A C T

This paper investigates biochemical, morphological and mechanical properties of a large range of plant fibres explored with the same methods. Biochemical results clearly exhibit strong differences between gelatinous, i.e. flax and hemp, and xylan type, i.e. jute and kenaf, cell walls. These differences into parietal composition have an impact on cell wall stiffness, highlighted through nanoindentation and atomic force microscopy measurements, but also on fibre individualisation, due to variations into fibre bundles cohesion. In addition, the morphology and particularly the lumen size induces apparent density differences. Moreover, the influence of fibre mor-phology and properties is demonstrated on UD materials. Finally, longitudinal Young's modulus of each plant fibre batches is back-calculated from UD stiffness by an inverse method; the results obtained are in accordance with the values in the literature values, proving the interest of this method to estimate longitudinal Young's modulus of short plant fibres.

Keywords:
Natural fibers
Biocomposite
Microstructures
Mechanical properties

1. Introduction

Nature offers a huge diversity of plant fibres; for their use in composite industry some key factors have to be considered. Regarding technico-economical data, price and availability of plant fibres are key issues, particularly for high volume industrial applications such as transport or building industry. Due to textile applications and important needs, flax fibres [1] are more expensive than glass ones [2], whereas high volume fibres, such as alfa, sisal or bamboo [3], are available at low cost in link with their low fibre quality, i.e. colour, length, mechanical properties or fineness. An intermediate group of fibres, including hemp and jute [4,5], represents an interesting compromise between performance and cost and can be considered as a good alternative able to fillers such as wood flour [6]. Localization of the fibre production is also an important parameter for final choice. Asian countries are leaders in the worldwide production of plant fibres production, particularly jute, coir and bamboo [2]. Nevertheless, other parts of the world have leading positions such as Brazil for sisal or France for flax. Despite their low volume on a global world scale, flax and hemp are mainly cultivated in Europe [2] and around 50% of the world production of these fibres is concentrated in France.

From a biological point of view, plant fibres are generally classified according to their location in plants [7]; they exhibit different functions and geometries, but also very diversified modes of growth that can explain differences into structural and morphological properties. In the case of primary phloemian fibres such as hemp or flax, the growth is well-described in literature. Main steps of the fibre development are characterized by first the cell multiplication [8], a first moderate coordinated elongation, a strong intrusive growth with cell wall structuring and finally a radial thickening [9]. During the intrusive growth, the fibre length increases of 5– 20 mm per day to a length of several tens of mm [9]. This extraordinary elongation, leading to remarkable length for single cell is allowed by multiplication of the nuclei along the cell [9]. Among the diversity of fibres, ramie fibres length can raise around 550 mm [10]; flax ones 40 mm [11–13] and hemp about 15 mm [9]. Finally, after this intrusive elongation begins the secondary cell wall

* Corresponding author.
E-mail address: alain.bourmaud@univ-ubs.fr (A. Bourmaud).

thickening by filling with cellulose and non-cellulosic polymers. In several plant species such as kenaf, hemp or jute, one can notice the apparition of secondary fibres, also developed with an intrusive mode and secondary cell wall thickening, but appearing latter than primary ones, produced by a cambium, and having a structuring and supporting function but a length of only few mm [2].

Besides these morphological differences, the functions of fibres within the plant induce major structural differences in terms of chemical composition, microfibrils angle (MFA) or lumen size. For fibres coming from annual stems such as hemp, flax, jute or kenaf, MFA values are generally included between 9 and 15° whereas they can be much higher when fibres originate from fruits or leaves [2]. The lumen size greatly varies according to the fibre origin, its area may represent only a few percent of the fibre whole cross section area for flax or hemp and can reach 30% for sisal, jute and even 60% for kenaf [2]. These structural parameters have a direct impact on apparent mechanical and hygroscopic performances of plant fibres [14].

Moreover, in addition to these structural differences, the biochemical composition of the fibres cell wall varies considerably according to the species, the method of cultivation or extraction mode of the fibres; thus the retting conditions are particularly influential on the composition of the fibre bundles, its action allowing to eliminate the common lamellae rich in lignin and pectins; if it is too prolonged it can also damage the structure of the secondary fibre wall [15]. It has been shown that these differences in biochemical composition can have an impact on the mechanical performance of plant fibres [16].

Thus, morphological, structural or biochemical properties of reinforcement fibres are key parameters that have a direct impact on composite performances. They can influence the fibre mechanical performances [17], the quality of the interface between fibres and matrix [18], the final microstructure of parts [19] and consequently the quality of the stress transfer between fibre and polymer matrix [20]. Besides these intrinsic parameters, exogenous ones such as thigmomorphogenesis [21], cultural practices [22] or environmental conditions [23] may also contribute to modify plant slenderness [24] and fibre properties and consequently structure and properties of associated composites.

The purpose of the present work is to explore the relationship between the origin and extraction conditions of plant fibres and performances of associated unidirectional composite. Four species of plant fibres, namely flax, hemp, jute and kenaf, originated from stems and industrially available, were selected. For flax, oleaginous flax fibres, flax tows as well as two qualities of long scutched fibres were chosen. These seven different fibre batches were firstly characterized in terms of biochemical composition, individualisation and water sorption behaviour. Then, unidirectional composite materials, made with epoxy matrix, were manufactured and tensile tested. Longitudinal fibre stiffness was estimated thanks to a back-calculation and mechanical performances of the composites were discussed according to the origin and the properties of plant reinforcements.

2. Materials and methods

2.1. Materials

Four types of flax (*Linum usitatissimum L*) were studied in this work; flax tows and long scutched flax fibres (Melina variety) obtained from Agylin (Normandy, France). Another quality of long scutched flax fibres were tested to compare with the previous one; thus, Eden, a flax variety known for its lodging resistance, was obtained from Terre De Lin (Normandy, France). Oleaginous flax tows (Solal variety) were cultivated and provided by the agricultural cooperative CAVAC (Pays de Loire, France). These four types of flax were all cultivated under normal meteorological conditions [25], dew-retted in fields and mechanically scutched in the same conditions; he plants were all grown during the same year and in neighbouring cultivation areas (Normandy, France). Hemp fibres (*Cannabis sativa L,* Fedora 17 variety) were supplied by La Chanvrière de l'Aube (Grand Est, France). Stems were mechanically harvested and dew-retted before hammer mill extraction. Jute (*Corchorus capsularis L*) and kenaf (*Hibiscus cannabinus L*) fibres, provided by Derotex (Wielsbeke, Belgium), were grown in Bangladesh, retted in water before being mechanically extracted from the stems. All fibres batches were cultivated in 2015, whatever their origin. An epoxy resin (Axson, Epolam 2020, density 1.2) was used as matrix. It was mixed with its amine hardener at 100:34 ratio.

2.2. Density measurements

The density of the different fibres was first determined by an immersion method in ethanol according to EN ISO 1183-1. A Mettler Toledo XS205 high accuracy weighing scale was used for the measurements. First, a low amount of fibres is weighted in the air and then introduced in ethanol until the weight stabilizes; density can then be calculated using:

$$\rho_f = \frac{m_{air}(\rho_{eth}-\rho_{air})}{m_{air}-m_{eth}} + \rho_{air} \quad (1)$$

where ρ_f,ρ_{air} (0.0012 g cm^{-3}), ρ_{eth} (0.7876 g cm^{-3}) represent fibres, air and ethanol densities at 22 °C, respectively.m_{air} and m_{eth} are the weight of the sample in air and in ethanol. For each type of fibres, weighing was repeated at least five times and the average of the measured values was calculated.

In addition, the fibres density was also determined by helium pycnometer. Prior to the measurements, the fibres were kept minimum 12 h at 21 °C and 50% RH. A Sartoruis R160D high accuracy weighing scale was used to get accurate mass value. Accupyc II 1340 gas pycnometer from Micromeritics™ was employed. Calibration was performed with a steel sphere before each series. The measurement is performed in two steps: 10 purge cycles and 30 measurement cycles. The density is obtained using the method described in ISO 1183-3 [26] standard with the following equation:

$$\rho_f = \frac{m_f}{V_{cel} - \frac{V_{exp}}{\frac{P_1}{P_2}-1}} \quad (2)$$

where m_f is he sample mass, ρ_f the sample density, V_{cel} the sample chamber volume, V_{exp} the expansion chamber volume, P_1 the gauge pressure after fill and P_2 the gauge pressure after expansion.

2.3. SEM analysis and estimation of the fibre elements individualisation

To enable the observation of their cross sections, fibres were embedded in an epoxy resin before polishing. Samples were then metallized with gold before being observed using a JEOL JSM 6460LV scanning electron microscope operated at an accelerating voltage of 20 kV. The sections of the fibres bundles are isolated on the SEM images using the GIMP® software and their areas were analysed with the ImageJ® software. A diagram describing the evolution of the cumulated frequency of fibre elements area is thus created. The coefficient of bundle individualisation is the ratio between the area under the cumulated frequency curve of the considered fibre element and the one corresponding to a perfect individualisation. The value of this coefficient is included between 0 and 1. The closer the value is to one, the more individualised the fibres are.

2.4. Monosaccharide analysis

The identification and quantification of neutral monosaccharide was carried out using high performance anion exchange chromatography in the manner described previously [27] but with slight modifications. The fibre elements fractions (approximately 1 g each) were cryo-grinded prior to hydrolysis. To do so, the sample powders were

obtained by milling individually the samples in a centrifugal grinding mill (Retsch ZM100) equipped with a 0.5 mm sieve, in liquid nitrogen to limit any heating effects. For hydrolysis, approximately 5 mg of each sample was immerged in 125 µL of 12 M H_2SO_4 acid for 2 h at room temperature and then the acid was diluted to 1.5 M and heat for 2 h at 100 °C. All samples were then filtered (PTFE, 0.22 µm) before being injected into a CarboPac PA-1 anion exchange column (4 × 250 mm, Dionex). Detection was performed by pulsed amperometry (PAD 2, Dionex) and samples were eluted using the following conditions: A (Milli-Q water) 95–0% with B (0.1 M NaOH in Milli-Q water) 5–100% for 19 min; then 100–0% B with C (0.3 M AcONa; 0.1 M NaOH in Milli-Q water) 0–100% for 49 min; and D 100% (0.3 M NaOH in Milli-Q water) for 6 min. A post-column addition of 0.3 M NaOH was used. Typical retention time obtained are 6; 15.5; 17; 21; 25; 31; 35; 51 and 51 min for Fucose (Fuc); Arabinose (Ara); Rhamnose (Rha); Galactose (Gal); Glucose (Glc); Xylose (Xyl); Manose (Man); Galacturonic Acid (Gal)A and Glucoronic Acid (GlcA) respectively. The monosaccharide composition was analysed and quantified using 2-deoxy-D-ribose as internal standard as well as three concentrations of standard solutions of neutral monosaccharides (L-arabinose, D-glucose, D-xylose, D-galactose and D-mannose) as calibration curves. Analyses were performed in three independent assays for every sample. The monosaccharide content is the sum of the amounts of the monosaccharides, and is expressed in two ways: as the percentage of the dry matter and as the percentage of the total carbohydrate.

2.5. Unidirectional composites manufacturing

Due to the small sample size, the fibres bundles used are short (80 mm) and it is quite simple to select straight ones for the manufacture of composites. There is no pre-tension applied to the fibres bundles at this stage. The amount of fibres bundles required to manufacture each composite is weighed and, then, they are manually aligned to form a unidirectional bundle. The bundle was then impregnated with the resin. The impregnated fibre bundle was then placed in an aluminium mould with open sections at each end to evacuate the excess of resin during compression. Given the small size of the mould section, the resin flow is mainly longitudinal and is assumed to have a reduced effect on mis-orientation [28]. After hardening at room temperature, 6 × 2 × 80 mm samples were post-cured following the resin supplier recommendations (3 h at 40 °C, 2 h at 60 °C, 2 h at 80 °C and finally 5 h at 100 °C) in order to complete the cross-linking of the resin. The volume fraction of fibres within the composites was set to 50% before the manufacturing and was then calculated by image analysis of composite cross sections. To prevent any slippage during tensile experiments, glass-epoxy end tabs were added to the specimens prior to tensile tests.

2.6. Mechanical characterization

2.6.1. Tensile tests on UD composites

Monotonic tensile tests were conducted on the unidirectional composites using an electromechanical testing machine INSTRON 5566A equipped with a 10 kN load cell. An INSTRON extensometer with a nominal length of 25 mm was used. Tensile tests were performed according to ISO 527 standard in controlled atmosphere in the laboratory (23 °C and RH = 50%). For each type of fibre, at least five samples were tested at a cross-head speed of 1 mm/min and the results were averaged arithmetically. The elastic modulus was calculated conservatively from the final portion of the stress–strain curve where stiffness is almost constant. This point has been deeply discussed elsewhere [29].

2.6.2. Atomic force microscopy investigations at the cell wall scale

Fibre elements were first dehydrated with a concentration series of ethanol/deionised water (50%, 75%, 90% and 100%) and then embedded in mixture containing increasing ratios of Agar epoxy (AGAR low viscosity resin kit, AGAR Scientific Ltd, Stansted, UK)/ethanol (25%, 50%, 75% and 100%) in order to maintain the fibre bundle and the cell wall structure during sample surface preparation. Final embedding resin polymerisation was carried out in an oven (60 °C, overnight). Then, the whole resin block with the sample is machined to reduce its cross section and an ultramicrotome (Leica Ultracut R) is used with diamond knives (Diatom Histo and Ultra AFM) to cut a series of very thin sections (about 50 nm thick in the last step) at reduced cutting speed (≈1 mm/s) to minimize compression and sample deformation during the cutting process. A commercial nanoindentation system (Nanoindenter XP, MTS Nano Instruments) was used at room temperature (23 ± 1 °C) with a continuous stiffness measurement (CSM) technique, equipped with a three-side pyramid (Berkovich) indenter. The system was operated at 3 nm amplitude, 45 Hz oscillations using a 0.05 s^{-1} loading rate. Measurements were taken at depths up to 120 nm. Around 20 indents were performed in each sample. In addition, mechanical characterization was performed by using a Multimode AFM (Bruker Corporation, USA) with Peak-Force Quantitative Nanomechanical property Mapping (PF-QNM) mode at 2 kHz. At each oscillation, the probe indents into the surface of the sample with a typical depth of 1 to 3 nm. RTESPA-525 (Bruker) probe was used. Its spring constant, around 200 N/m, was calibrated using the so-called Sader method [30], with a Scanning Electron Microscope (Jeol JSM 6460LV) for the measurements of the cantilever length and width, and the AFM in Tapping™ mode, for the measurement of its frequency response (resonance frequency and quality factor). The applied maximum load (peak force) is set to 200 nN for all the measurements, leading to a contact stiffness of the same order as the cantilever stiffness for the studied materials [31]. The calibration was checked by comparing values obtained with those of nanoindentation.

3. Results and discussions

3.1. Investigations at the reinforcement scale

3.1.1. Study of the biochemical composition of plant fibres

First of all, for the biochemical composition of the plant fibres used, some components are in very low quantities. To measure such low quantities, such as Fucose, we used an HPAEC-PAD analytical system to increase in sensitivity [32]. Table 1 shows the results of biochemical composition analysis for each sample. These values are averaged from 3 separate analyses.

Interestingly, one can notice that the total polysaccharide content is in the same range, almost 3/4 of the dry matter whatever the plant species. In this study, all fibres come from bast fibres that are supporting tissues within the plant and, although this point can be moderate for jute and kenaf, with fibres coming from bark but also of core (wood/xylem) area [33], the relationship between function and overall polysaccharidic content can be underlined. The total amount of polysaccharides is included between 71.8 ± 3.7% for flax tows and 79.5 ± 2.4% for jute fibres, which is similar to values reported for similar plant varieties in the literature [7,34–36]. Slight variations between the different batches may be linked to the particular history of each plant batch (e.g., growth, environmental stress). Other components of dry matter are probably lignin, proteins, waxy-lipids or minerals; they were not quantified during this work.

Whatever the plant species, the main component is glucose, which is often associated to para-crystalline cellulose and representing between 79% and 87% of the whole monosaccharides (Table 1: ratio between glucose content and total of monosaccharides). One can notice lower glucose content for jute and kenaf fibres, which is also in good agreement with literature data [37]. Whatever for jute or kenaf, within the plant; fibres are arranged in bundles of several tens located along the radial section of the stem, from the cortex to the cambial zone. As illustrated in Fig. 1, with examples of cross sections of flax, hemp, jute and kenaf stem, plant fibres may come from different tissues. The function of these latters differs. Some of them ensuring a role of

Table 1
Biochemical composition of the different plant fibre batches. Fuc, Ara, Rha, Gal, Glc, Xyl, Man, GalA and GlcA represent the fucose, arabinose, rhamnose, galactose, glucose, xylose, manose, type A-galactan and type A-glucose contents. All values are expressed in percentages of dried matter.

	Monosaccharides									Total monosaccharides	Non glucosidic monosaccharides
Fibre origin	Fuc	Ara	Rha	Gal	Glc	Xyl	Man	GalA	GlcA		
Kenaf	0.04 ± 0.01	0.28 ± 0.01	0.27 ± 0.01	0.53 ± 0.01	60.5 ± 0.2	13.1 ± 1.22	0.97 ± 0.95	0.85 ± 0.21	0.21 ± 0.03	76.9 ± 1.6	16.3
Jute	0.04 ± 0.01	0.24 ± 0.01	0.29 ± 0.01	0.60 ± 0.01	62.7 ± 1.1	13.5 ± 1.07	0.93 ± 0.15	0.90 ± 0.20	0.26 ± 0.04	79.5 ± 2.7	16.7
Hemp	0.06 ± 0.01	0.62 ± 0.01	0.52 ± 0.11	2.39 ± 0.27	64.6 ± 1.3	1.57 ± 0.15	5.52 ± 0.60	1.27 ± 0.39	0.19 ± 0.02	76.8 ± 2.8	12.1
Melina flax tows	0.08 ± 0.01	0.51 ± 0.01	0.41 ± 0.01	2.61 ± 0.24	60.3 ± 3.3	3.67 ± 0.26	3.19 ± 0.37	0.96 ± 0.12	0.08 ± 0.01	71.8 ± 3.7	11.5
Solal flax fibres	0.11 ± 0.01	0.65 ± 0.01	0.39 ± 0.07	3.06 ± 0.34	58.2 ± 3.1	3.53 ± 0.36	4.51 ± 0.36	1.41 ± 0.41	0.08 ± 0.01	72.0 ± 4.9	13.7
Eden Flax fibres	0.06 ± 0.01	0.36 ± 0.01	0.37 ± 0.04	3.55 ± 0.41	64.9 ± 2.9	0.89 ± 0.09	3.79 ± 0.24	0.78 ± 0.13	0.05 ± 0.01	74.7 ± 3.9	9.88
Melina flax fibres	0.07 ± 0.01	0.47 ± 0.01	0.41 ± 0.08	3.42 ± 0.40	65.7 ± 2.4	0.89 ± 0.10	3.66 ± 0.35	0.82 ± 0.15	0.06 ± 0.01	75.5 ± 3.6	9.82

Fig. 1. Schematic drawing of a part of flax, hemp, jute and kenaf stem cross section; fibres are evidenced in red colour. (For interpretation of the references to colour in this figure legend, the reader is referred to the web version of this article.)

conduction of the raw or elaborated sap, others being composed only by fibres intended to support the stem and ensure its stability. For kenaf, fibres are located in the bast (cortical layer) and core (wood) region. The bast ones constitute around 40% of the total fibre amount. In case of jute the presence of two types of fibres was also demonstrated [38]. Both primary phloic fibre (PPF) from procambium in the protophloem region and secondary phloic fibre (SPF) from cambium are developed. In a mature jute plant, PPF and SPF account for about 10 and 90% of the total fibre fraction [39]. Thus, for kenaf but also for jute, the chemical composition of the fibres is highly dependent on the tissue from which they come. The lower glucose level observed for jute and kenaf can be explained by possible mix between primary and secondary fibres in our batches. A lower glucose amount is also noticed for oleaginous Solal flax, previous works have highlighted some differences between biochemical composition of textile and oleaginous flax. For example, Alix et al. [40] estimated a cellulose content of 84% and 77% for Hermes textile variety and Oliver oleaginous one, respectively.

To go further and better analyse the monosaccharide composition of the different plant cell walls, Fig. 2 details the parietal composition without the glucose component. Interestingly, the distinction between xylan and gelatinous cell wall is highly demonstrated, especially regarding the xylose content in jute and kenaf cell walls, which is significantly higher than for hemp or flax fibres. Due to higher lumen size, jute and kenaf fibres contain more important fraction of primary cell wall expressed relatively, which are enriched in xylose compared to other layers. Moreover, conduction fibres originating from stem core

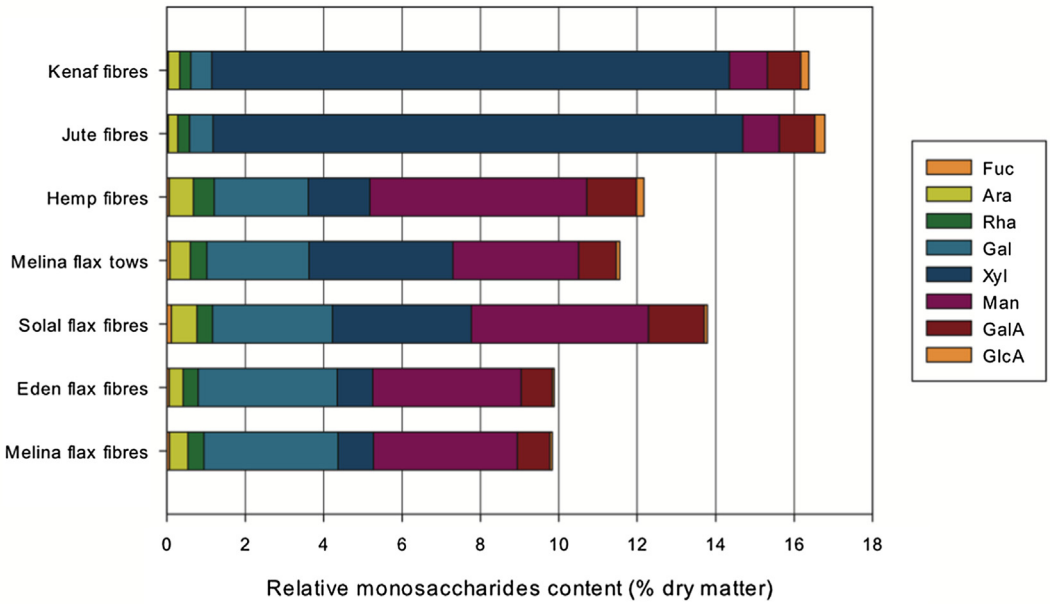

Fig. 2. Monosaccharide composition of the different plant fibres elements (excepted Glc). Results are expressed relatively to dry matter content. (For interpretation of the references to colour in this figure legend, the reader is referred to the web version of this article.)

may exhibit higher xyloglucan content. On the other side, flax and hemp cell walls exhibit high gelatinous components such as arabinose, rhamnose, galactose and mannose. Thus, the composition of the walls also varies according to the species considered, Mikshina et al. [41] propose a classification making it possible to differentiate gelatinous fibres rich in cellulose (flax and hemp for example) from xylane-type fibres, enriched in xylose and lignin and lower in cellulose (wood or jute). Galactose fraction is significantly higher for flax compared to hemp and especially to jute and kenaf; as underlined by Beaugrand et al. [27]. Galactose content can be linked to the cell wall or fibres mechanical performances as well as arabinose, thanks to the involvement of these two monosaccharides in structuring hemicelluloses building. One can notice the very strong reproducibility into biochemical composition of Melina and Eden long scutched fibres, proving the high degree of quality and scutching of these two batches, being free of impurities such as residual shives or cortical components. This point is underlined if we look at Melina tows or oleaginous Solal fibres. Due to a lower scutching degree and potential pollution of the batches with shives and dust particles, xylose fraction, coming probably from residual shives, is significantly higher. Finally, if we consider hemp composition, the main difference with flax is the high mannose and GalA (Galacturonic acid) contents. These two components are preferentially located in primary cell wall and also in middle lamella for GalA; it can be an indication of lower retting degree for our hemp sample with remaining middle lamella fractions. Finally for hemp bast fibres, an interesting comparison could be done with a recent paper from Liu et al. [42]. Those authors quantified the hemp monosaccharide in non-retted bast fibres and in treated ones by biological depectinization in the laboratory with the help of a lignocellulosic decomposer (white rot fungi). This treatment is expected to result in a modification of pectin, as the dew retting impact. If we compare the arabinose (Ara), GalA and other monosaccharides, we face globally a very comparable content.

3.1.2. Density of the plant bundles walls

Fig. 3 shows the average densities measured for the different plant reinforcements studied during this work; data were obtained thanks to both liquid (ethanol) immersion method and gas (helium) pycnometer.

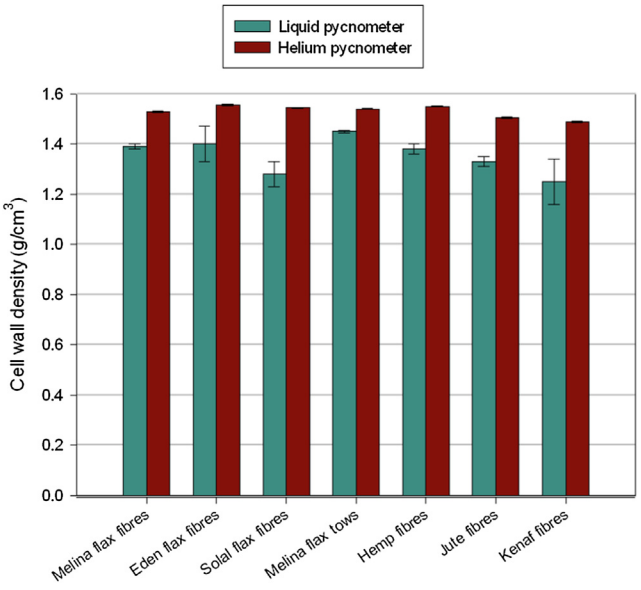

Fig. 3. Average density of the different plant fibres bundles obtained by liquid immersion and gas pycnometer methods. (For interpretation of the references to colour in this figure legend, the reader is referred to the web version of this article.)

Regarding liquid immersion measurements, significant variations are noticed according to the nature of the fibres studied. The value usually used for the density of the plant cell walls is 1.54 g/cm^3 [43] but the apparent density of the fibre may be very different mainly depending on the size of the lumen that may influence the filling of this latter by the ethanol used for the measurement, the length of the fibres or their state of retting. In fact, the presence of pectic compounds with a high affinity for water may distort the measurement. For flax fibre, our density measurements range from 1.28 g/cm^3 to 1.43 g/cm^3. These values are consistent with data from the literature, which generally range between 1.28 g/cm^3 [44] and 1.53 g/cm^3 [45]; the large variations noted can be explained by the absence of a standardized method but also by

differences in morphology between the different varieties. However, the values obtained on oleaginous Solal flax are much lower than those obtained on the three lots of textile flax. As can be seen in Fig. 3, oleaginous Solal flax fibres have much more pronounced lumens than textile flax varieties, which can influence the measurements, as the liquid used during the measurement has difficulty in penetrating the whole lumens. The measured densities are then more apparent fibre densities than wall densities. In addition, the retting level of this flax may be lower and residues of middle lamellae or shives may alter the measured density value. For the other fibres studied, the values are of the same order of magnitude as the data in the literature, whether for hemp, kenaf or jute [2]. The lower values observed on kenaf and jute can also be explained by the large lumen sizes, especially for kenaf, but also by the differences in biochemical composition, these walls being less rich in cellulose, which is the densest component among the plant's cell walls.

In addition, measurements with helium pycnometer were performed, results are showed in Fig. 3. Interestingly, a significant difference is shown between helium pycnometer and liquid immersion measurements with double weighing in ethanol. Due to the ease with which helium can penetrate cell wall porosities and in particular lumens, the density values obtained by helium pycnometer are higher than those obtained by liquid immersion means. The difference between the two densities is between 6.2% and 20.6% depending on the type of plant considered. The lowest values are obtained with textile fibre flax, which has the smallest lumens, and the highest with kenaf and oleaginous flax, both of which having significant lumens (Fig. 4). Surprisingly, the difference is more reduced with jute fibres, for which, despite a rather pronounced lumen size, the difference between the two densities is only 13.1%. This can be explained by the short length of the fibres and their structuring into cohesive bundles, which probably makes it more difficult for gas to penetrate the core of all lumens. Finally, it is interesting to note that the density values obtained by gas pycnometer are all very similar, whatever the plants considered, they are between 1.489 ± 0.004 and 1.554 ± 0.004. This result shows that, whatever the biochemical composition of the walls, their densities are close, which confirms that the densities of their constituents are similar [46]. The use of two methods also shows the limits of certain techniques [47]; liquid immersion measurements make it possible to obtain apparent fibre densities whereas by using gas pycnometer, it is possible, depending on the morphology of the fibres, to approach the true density of the plant fibre walls.

3.1.3. Estimation of the plant fibres individualisation within UD composites

Fig. 4 shows observations of the cross-sections of the different fibres elements through scanning electron microscopy. We can see significant differences in the filling rate of the cell walls between the fibres species. The fibres from the long scutched fibre (Fig. 4.a and 4.b) have a well hexagonal geometrical shape and reduced lumens dimensions. These fibres therefore possess a morphology that is favourable to obtaining good mechanical properties.

The Melina flax tow fibres (Fig. 4.c) and even more the oleaginous Solal flax fibres (Fig. 4.d) have a flatter cross-section that indicates insufficient secondary cell wall filling, so we can expect lower performance. Oleaginous flax is a plant mainly grown for its seeds. The transformation of its fibres into nonwovens is part of a process to valorise the co-products of the seed. Hemp fibres (Fig. 4.e) have a fairly irregular cross-section and variability in filling rates, which has been already demonstrated by various authors [17,48]. Moreover, these fibres can be obtained from primary or secondary fibre areas depending on the size of the stems and the areas of removal in the plant [48], which can lead to a significant scattering in the morphology of the fibres, the ones issue from the secondary fibres area having significantly smaller diameters. Finally, the kenaf and jute fibres (Fig. 4.f and g) have a larger lumen but highlight an apparent regular cross-section geometry.

Whether carried out in the field (for flax and hemp) or in water (jute and kenaf), the control of retting is a key point for optimal fibre preparation. For flax and hemp, the purpose of retting is to degrade the middle lamellae (to improve the separation of the bundles), while for kenaf and jute it is used to facilitate the extraction of the bundles of fibres from the stem. For flax and hemp, one of the major consequences of an incomplete retting is the important presence of remaining middle lamellae that prevents a good separation of the bundles [49]. To achieve optimum stress transfer between the fibre and matrix in the composite by maximizing the contact surface, it is important to use well-divided fibre bundles and to remove non-adherent residues of middle lamellae on fibre surface, which act like drawbacks. Moreover, a limited amount of middle lamellae reduces the size of the bundles in width and improves the homogeneity of the fibre material. For kenaf and jute, lignin acts as a link between the elementary fibres and also promotes fibre/matrix adhesion [50]. In order to use plant fibres as reinforcements for composite materials, the impact of retting on the individualisation of fibres can be studied by taking into account their botanical origin as well as the extraction route.

Fig. 5.a shows the evolution of the surface distribution of fibre elements and Fig. 5.b the individualisation coefficients calculated for each fibre type. The higher the coefficient, the higher the individualisation. We note that jute, kenaf and hemp fibres exhibit the lower individualisation values; these three types of fibres have a higher lignin content than flax, particularly in the region of middle lamellae, making the fibre bundles more cohesive and more difficult to separate. On the other hand, the bundles of flax fibres, whether long fibres or tows, are already very divided, the division having probably been carried out during the scutching process, facilitated by an optimised retting process.

By comparing the individualisation coefficients of the different fibre types, two main groups of morphologies can be distinguished. On the one hand, reinforcements with a good division (tows and long flax fibres) and, on the other hand, bundles that are more lignified and therefore more cohesive and can be divided less easily (hemp, kenaf, jute). The greater amount of lignin present in the bundles of hemp, jute and kenaf fibres [33] may be due either to the late harvest date for hemp or to the composition of the walls for kenaf and jute. The flax fibres have undergone a retting process that has allowed to degrade the middle lamellae (enriched in pectin) and thus to improve the individualisation of the bundles.

3.1.4. Comparison of plant cell wall indentation modulus

Fig. 6 shows nanoindentation and AFM PF-QNM indentation modulus values obtained on the different plant cell walls. In this work, nanoindentation tests are performed with the objective to validate the AFM PF-QNM values which are more arguable due to the low investigation depth within the cell walls (only few nm).

Generally speaking, the nanoindentation tests conducted in the plant cell walls yield a longitudinal indentation modulus between 15 and 22 GPa [2]. These values are difficult to compare with apparent longitudinal modulus obtained by tensile tests on elementary fibres because of the scale of investigation and the non-uniaxial loading nature of indentation, especially enhanced for anisotropic material [51]. Thus the resulting modulus is generally an intermediate value between transverse and longitudinal one, the plant fibres having a high degree of mechanical anisotropy [52,53]. The values obtained in our case are consistent with the data from the literature cited above; they are included between 17.5 ± 2.4 GPa for jute fibres and 23.9 ± 2.4 GPa for Eden flax fibres. Regarding the nanoindentation modulus, our values are in the same range than flax, jute or hemp fibres studied in a previous study [54]. Nevertheless, some significant differences exist and two main groups can be distinguished, the first one, with high indentation modulus values, concerns textile flax and hemp cell walls and the second includes oleaginous Solal flax, jute and kenaf with lower indentation modulus values. Variations between plant

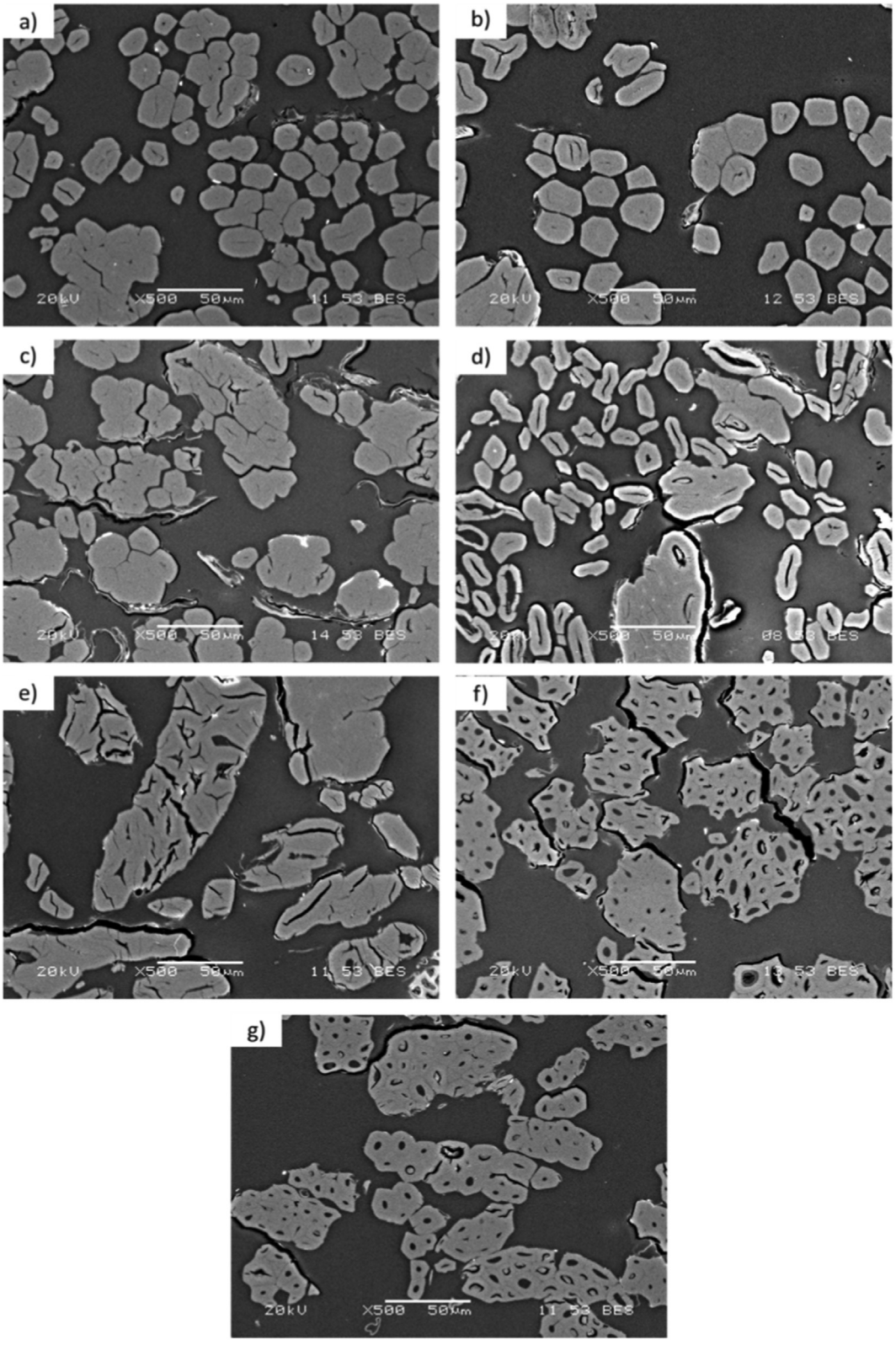

Fig. 4. SEM observation of fibres bundles' cross sections of Melina flax fibres (a), Eden flax fibres (b), Melina flax tows (c), Solal flax fibres (d), hemp (e), kenaf (f) and jute (g).

varieties may be induced by variation into the microfibril angle (MFA) of the crystalline cellulose or by the cellulose to matrix volume ratio. As described in Eder et al [51], the indentation modulus is not mainly linked to the cellulose properties, and to their microfibrillar angle, but to the cell wall matrix properties too, due to the high sensitivity of the indentation modulus to both transverse modulus and shearing stress.

The nanoindentation test can be considered relatively macroscopic at the plant wall scale, with an investigation volume of a few micrometres square in our case. It cannot provide a fine analysis at the monosaccharide, but the response may vary depending on the

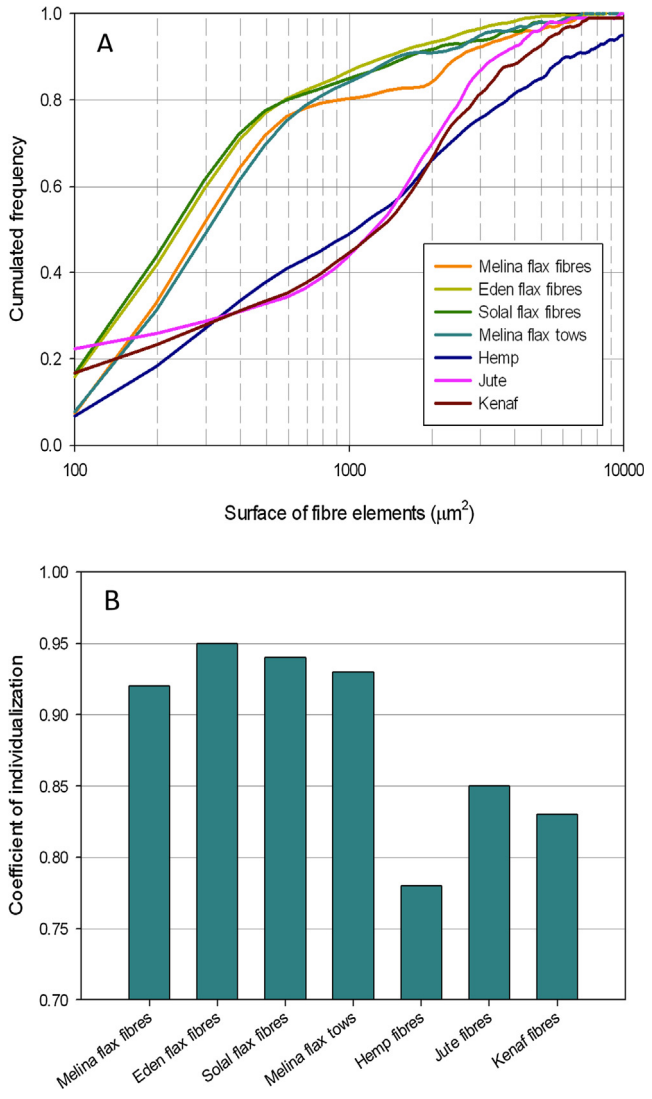

Fig. 5. Cumulated frequency of fibres cross sections (A) and coefficient of individualisation (B) for each fibre reinforcement. (For interpretation of the references to colour in this figure legend, the reader is referred to the web version of this article.)

crystalline cellulose content of the plant cell walls investigated. Here, the two populations identified in terms of indentation modulus are also distinguished by their glucose content, which is a representative marker of the amount of β-Glucan in cell wall, arguably cellulosic and mostly crystalline in the fibre plant cell walls studied. Table 2 thus clearly shows lower cellulose content for jute, kenaf and oleaginous Solal flax. These nanoindentation data were supported by an AFM PF-QNM analysis at the cell wall scale. Fig. 7 proposes example of PF-QNM indentation modulus mapping at the cell wall scale for Eden flax, hemp and kenaf fibres. One can notice, there are undulations in the indentation modulus map of kenaf. They are caused by interferences from the incident AFM laser and its reflection on the sample surface [55]. It induces a bias in the measurement of the adhesion force that is taken into account in the computation of the indentation modulus. In our case, for these measurements, nothing could be done to reduce or remove them, but this bias does not change our analysis of the average behaviour of the cell wall. Firstly, one can notice a good correlation between the two investigation ways (Fig. 6). The S2 layers indentation modulus values obtained by PF-QNM are very close to those obtained by nanoindentation with low difference between the two measurement methods whatever the fibre studied. AFM PF-QNM indentation modulus

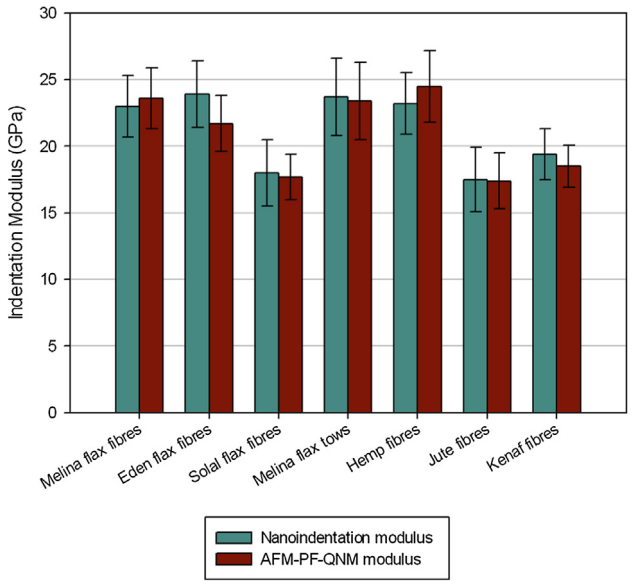

Fig. 6. Nanoindentation and AFM PF-QNM indentation modulus of the plant cell walls. (For interpretation of the references to colour in this figure legend, the reader is referred to the web version of this article.)

values are in good agreement with similar measurements on flax, and jute or kenaf data are similar to previously values measured on palm cell walls [2]. The significant differences in terms of indentation modulus are confirmed in AFM PF-QNM, which proves that the mechanical performance of the secondary cell wall is linked to the plant's genetic pool and the biochemical architecture of the walls, which differs between the two varieties [40]. One can observe a larger lumen in the kenaf fibres but this consideration must be moderated given the small area of investigation, which is not necessarily representative of the whole lot. Finally, there are significant morphological differences in the middle lamella between the fibres. In the case of Eden flax, it is very thin and much thicker for hemp and kenaf. It has a morphology comparable to that already observed on hemp fibres [48]. The degree of significant lignification in these areas is probably an influential factor in this morphology. In the case of flax, the extraction and senescence of the plant occurs before this lignification takes place. In this section, PF-QNM and nanoindentation experiments were combined to investigate the cell wall mechanical performances of our different plant fibre batches. Interestingly PF-QNM confirms nanoindentation values and gives pertinent information in terms of cell wall bundles structure and morphology.

3.2. Investigations at the composite scale

3.2.1. Longitudinal tensile properties on UD composites

Table 2 synthetizes results of the tensile mechanical properties as well as porosity content and fibre volume fraction. The porosity content was calculated from SEM images similar to Fig. 4 ones. Four images were analysed for each sample thanks to ImageJ® software and an automatic calculation of the degree of porosity. Average values of porosities are reported in Table 2. Fibre volume fraction was obtained considering the porosity degree of each sample with:

$$V_f = \frac{\rho_c + \rho_m.(V_p - 1)}{\rho_f - \rho_m}, \quad (3)$$

where ρ_c, ρ_m and ρ_f being the density of composite, polymer matrix and fibres, respectively and V_p the porosity volume fraction. We considered the fibre density obtained with liquid immersion method in order to take into account the apparent density of fibre and not the true density of the cell walls.

Table 2
Mechanical properties of unidirectional plant fibre composites.

Fibrer origin	Young's Modulus (GPa)	Strength at break (MPa)	Strain at break (%)	Porosity content (%)	Fibre volume fraction (%)	Estimated fibre modulus (GPa)
Kenaf	17.9 ± 1.3	202 ± 28	1.07 ± 0.15	1.16 ± 0.13	51.6 ± 1.2	32.6 ± 9.6
Jute	21.6 ± 1.3	195 ± 11	0.91 ± 0.09	0.92 ± 0.08	51.4 ± 0.9	39.9 ± 7.5
Hemp	14.2 ± 1.8	222 ± 9	1.49 ± 0.08	1.12 ± 0.27	58.2 ± 1.3	22.7 ± 2.2
Melina flax tows	21.8 ± 1.4	310 ± 22	1.35 ± 0.16	0.83 ± 0.11	53.5 ± 0.8	38.7 ± 4.0
Solal flax fibres	13.3 ± 1.6	190 ± 38	1.28 ± 0.15	0.91 ± 0.08	49.4 ± 0.8	26.9 ± 3.1
Eden Flax fibres	29.7 ± 1.8	303 ± 55	1.11 ± 0.13	0.65 ± 0.10	52.6 ± 0.7	59.0 ± 5.2
Melina flax fibres	24.8 ± 4.0	302 ± 62	1.26 ± 0.12	0.78 ± 0.15	48.7 ± 0.6	48.5 ± 3.2

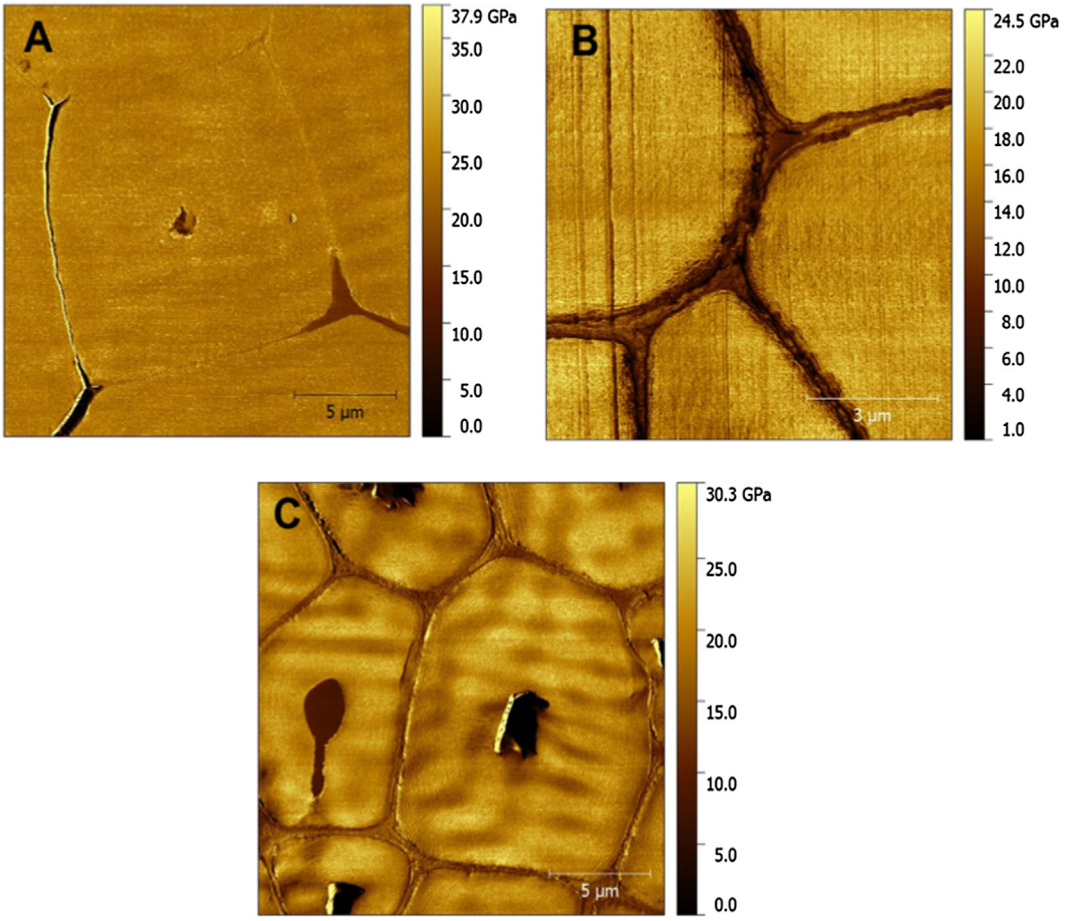

Fig. 7. Example of AFM PF-QNM indentation modulus map of Eden flax (A), hemp (B) and kenaf (C).

Fig. 8 shows the tensile mechanical behaviour of the different plant fibres unidirectional composites; values for apparent modulus, strength and strain at break are detailed in Fig. 9. The curves selected are representative of average tensile behaviour for each sample. As expected, and whatever the plant fibre considered, a non-linear behaviour is highlighted [28] with two distinct slopes on the stress-strain curves separated by an inflection point corresponding to the beginning of the plant fibres microfibrils reorganisation. The considered fibres exhibit very close MFA. Values for flax, hemp, jute and kenaf being included between 8° and 15° Due to this particular behaviour, the pertinent area for modulus calculation is questionable in the case of plant fibres UD. As evidenced by Shah [29] and Bourmaud [56], UD plant fibre composites exhibit significant instability and a drop of stiffness up to an applied strain of 0.4% (Fig. 8), which suggests that the initial stiffness is probably not conservative enough. After this decrease, stiffness remains quite stable with a moderate improvement until the composite failure. In this work, apparent modulus calculation were performed in the second part of the curve; Bourmaud et al. [56] demonstrated, on PA11-flax UD, that this stiffness value is very similar to the rule of mixture prediction, whatever the fibre volume fraction considered and can be assumed to be the more pertinent for UD. Fig. 10 compares the Young's modulus and strength at break of epoxy/plant fibres composites with literature data. One can notice a suitable correlation between the fibres volume fraction and the composites Young's modulus or tensile strength. Indeed, the properties of the unidirectional composites are mainly influenced by the mechanical performance of the reinforcement. Mechanical properties of Eden and Solal Flax fibres are well correlated with literature data. Same conclusion can be notice for flax tows epoxy composite, especially for strength value that is fully in line with literature values for different fibres loading rate. These three batches of composites exhibit similar strength values (Fig. 9); the stiffness is slightly lower when flax tows are used, probably due to the fibre length and consequently to the lower fibre aspect ratio. Regarding the composite strength, this parameter is generally highly positively impacted by the fibre individualisation, which is suitable whatever the considered fibre batch.

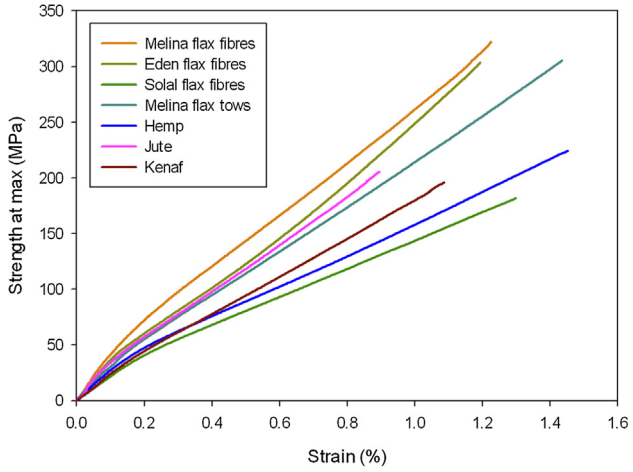

Fig. 8. Stress-Strain tensile behaviour of the unidirectional epoxy-plant fibres composites. The curves selected are representative of average tensile behaviour for each sample. (For interpretation of the references to colour in this figure legend, the reader is referred to the web version of this article.)

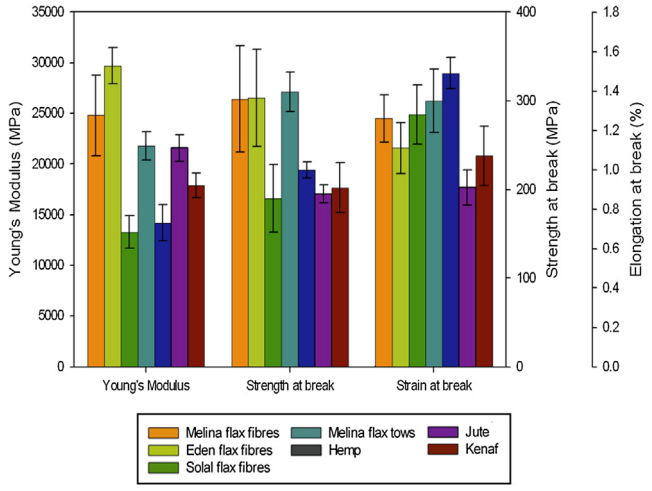

Fig. 9. Tensile modulus, strength and elongation at break of the unidirectional epoxy-plant fibres composites. (For interpretation of the references to colour in this figure legend, the reader is referred to the web version of this article.)

Mechanical values of composites reinforced with oleaginous flax fibres exhibit lower stiffness and strength values compared to other flax samples. This assessment is consistent with indentation modulus obtained from AFM investigation and also with the cell wall thickening, which is very low compared to other batches of flax. The low cell wall thickness and stiffness fully explain the lower mechanical values of the associated composites. These fibres were grown in a region located further south of France, which does not have climatic conditions as favourable for flax cultivation as Normandy; the quality of the soil can also be different. The combination of these environmental parameters can lead to cells with a lower cellulose content, less mature but also with a shorter length, which penalizes the performance of the associated composites [23]. In addition, the quality of the retting can also be impacted and influences the performance of the fibres [49]. The wall stiffness measured by AFM, very low compared to those of the other flax samples, indicate a sub-maturity of these fibres in terms of structuring of the main cell wall constitutive polymers, this non cellulosic polymer architecture having an impact on cell wall mechanical performances [40]

Composites reinforced with hemp fibres exhibit also very low performances regarding the considered fibre volume fraction. The poor exhibited performances (Fig. 9) can be explained by differences in terms of biochemical composition; as underlined before, galactose fraction is significantly higher for flax compare to hemp. It has been showed that galactose is one of the main monosaccharides involved in the architecture of structuring hemicelluloses that have a major role on fibre's mechanical performances [27]. Moreover, one can notice that hemp fibres are the less individualised of the seven batches considered which also strongly penalizes the reinforcement of composite, middle lamellae within bundles being potential weak areas. This statement is probably linked to a sub-retting of hemp fibres. Nevertheless, the epoxy-hemp composite UD performances are consistent with literature data (Fig. 10). Interestingly, one can notice that hemp composite performances, in term of stiffness and strength at break (blue points in Fig. 10), are similar to flax ones for low fibre volume fraction but a significant drop appears from 50% fibres volume fraction. This behaviour can be linked to problems into impregnation induced by the packing of the fibres for high fibre fraction and the significant fraction of middle lamella; the maximal reachable reinforcement ratio, i.e. packing factor being thus penalized.

Finally, composite properties of kenaf and jute reinforced composites are shown. The associated composites exhibit lower properties compared to flax ones but in the same range of hemp. Interestingly, our results are well correlated with literature ones, especially for kenaf. Low performances may be explained by the short fibre length and the important bundle cohesion leading to poor individualisation (Fig. 5), as well as by the moderate cell wall stiffness (Fig. 6).

3.2.2. *Estimation of plant fibres stiffness*

Having the mechanical properties of UD composites, it is possible to back calculate the fibre's stiffness thanks to a Rule Of Mixture (ROM) modified by Madsen et al. [57]:

$$E_{L,UD} = (E_{L,f} \times V_f + E_m \times V_m).\ (1 - V_p)^2 \tag{4}$$

$$E_{L,f} = \frac{E_{L,UD}.(1 - V_p)^{-2} - V_m \cdot E_m}{V_f} \tag{5}$$

where $E_{L,UD}$, $E_{L,f}$, and E_m are the tangent modulus of the unidirectional composite, of the elementary fibre and of the polymer matrix, respectively, and V_f, V_m and V_p the volume fraction of fibre, polymer matrix and porosities, respectively. If significant differences exist between experimental and calculated fibre's strength, generally due to quality of interface and fibre's individualisation [58], we can assume that it is relevant to estimate the longitudinal fibre modulus, a good correlation being generally noticed between fibres and composite stiffness. Fig. 11 gives the synthesis of these calculations for each fibre batch. As expected, the scutched flax fibres exhibit the better stiffness, the values obtained are well correlated with literature data for textile varieties [59]. Estimated stiffness is significantly lower for Solal fibres and Melina tows; one can notice from biochemical results that these two batches exhibit some fractions of woody core as evidenced by high xylose and mannose content; these components penalize the composite stiffness by creating weak areas. Moreover, the relatively low cell wall thickness of the oleaginous fibres also explains the low fibre performances. Regarding hemp, kenaf and jute stiffness, the estimation of the fibre stiffness is in line with literature results both for elementary fibre tests [2] and for back calculation from composite characterization [60].

4. Conclusion

In this study, biochemical compositions, apparent densities, degrees of individualisation and mechanical performances at the cell wall scale of a wide range of plant fibres were explored. Thus, textile flax, oleaginous flax, flax tow, hemp, kenaf and jute fibres elements were characterized using the same techniques and protocols. The biochemical compositions showed significant differences, particularly in terms of glucose, xylose, mannose and galactose content, making it possible to

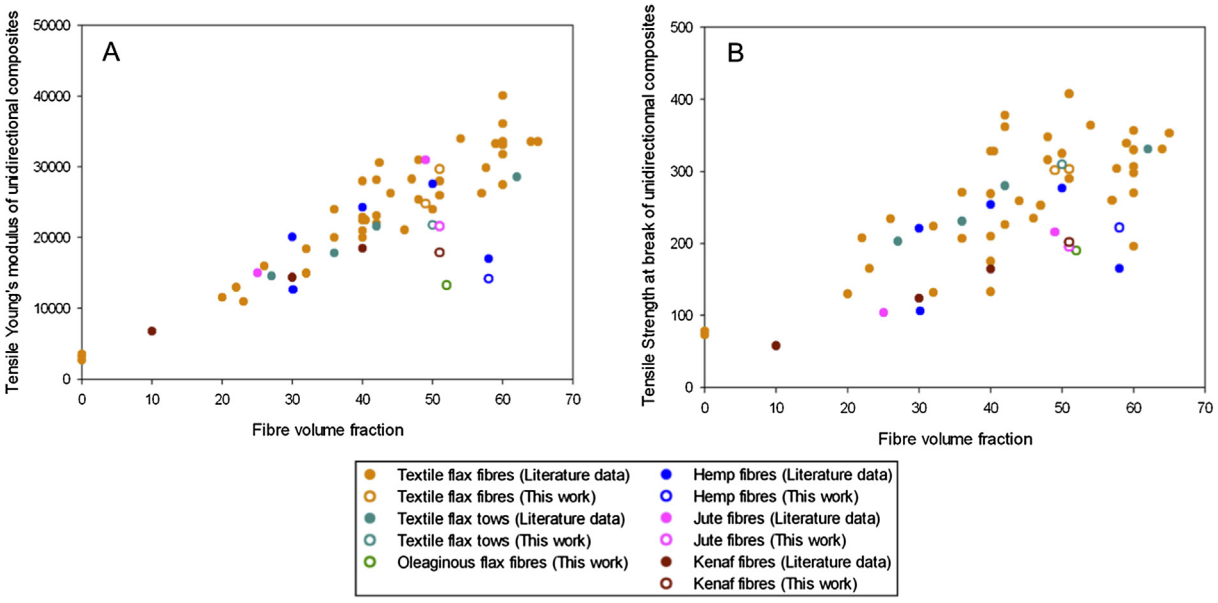

Fig. 10. Young's modulus (A) and strength at max (B) of plant fibres epoxy composite in comparison with literature data. (For interpretation of the references to colour in this figure legend, the reader is referred to the web version of this article.)

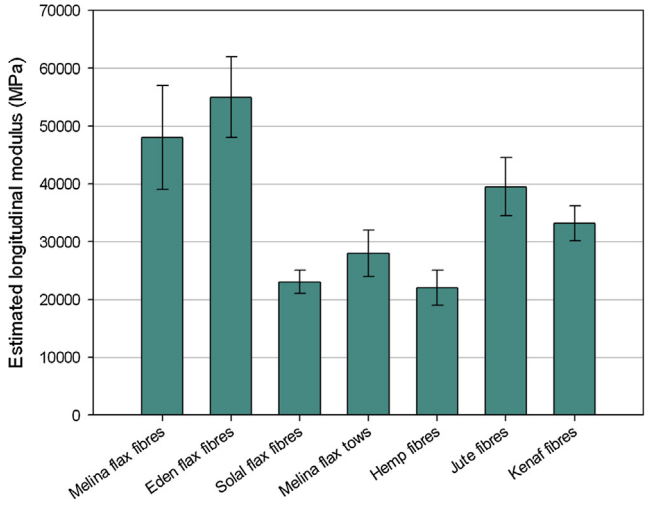

Fig. 11. Estimated longitudinal modulus of plant fibres. (For interpretation of the references to colour in this figure legend, the reader is referred to the web version of this article.)

differentiate gelatinous fibres (flax and hemp) from xylose fibres (jute and kenaf) types. These differences are linked to the botanical origin of the fibres and also to their function in the plant. This biochemical composition, and in particular the galactose content, which is a structuring polymer of the cell walls, plays a major role on the mechanical performance; this has been demonstrated by nanoindentation and atomic force microscopy tests. In addition, biochemical architecture of middle lamella impacts the individualisation capacity of the bundles. The morphology of the cell, and in particular the size of the lumen, also has an impact on the apparent density of the fibres and consequently on those of the associated composites. This was confirmed by tensile tests conducted on epoxy-plant fibre UD composites. The latter also highlighted the importance of fibre length, bundle cohesion and fibre individualisation on the mechanical properties of composites. The last section of the study focuses on the calculation of the stiffness of the different fibres studied using an inverse method, knowing the volume fractions and Young's moduli of the UD composites produced. The performances obtained are consistent with the literature data; they confirm the use of this method to estimate the longitudinal properties of the fibres that are too short to be tested in tension, such as jute and sisal.

Declaration of Competing Interest

The authors declare that they have no conflict of interest that could have appeared to influence the work reported in this paper.

Acknowledgements

The authors want to acknowledge the OSEO Agency, Région Bretagne, the French research cluster CNRS-INRA 'Symbiose' SYnthon et Matériaux BIOSourcés, the PSPC collaborative projects FIABILIN and SINFONI and the French Research Ministry for funding this work. Francois Gaudard, Sylviane Daniel and Audrey Geairon (INRA) are also thanked for his technical assistance in HPLC.

Bibliography

[1] SANECO. Prix moyen annuel (FOB) des fibres de lin teillées; 2015.
[2] Bourmaud A, Beaugrand J, Shah DU, Placet V, Baley C. Towards the design of high-performance plant fibre composites. Prog Mater Sci 2018;97:347–408. https://doi.org/10.1016/j.pmatsci.2018.05.005.
[3] Food and Agriculture Organisation of the United Nations (FAO). Future fibres. Futur Fibres 2015. http://www.fao.org/economic/futurefibres/prices/en/.
[4] Dittenber DB, GangaRao HVS. Critical review of recent publications on use of natural composites in infrastructure. Compos Part A Appl Sci Manuf 2012;43:1419–29. https://doi.org/10.1016/j.compositesa.2011.11.019.
[5] Institute N, Nova Institute. Price index: hemp and flax technical short fibres. Nov Inst; 2012.
[6] Ekstroem H. The North American Pulpwood and biomass market this quarter. North Am Wood Fiber Rev 2018.
[7] Jawaid M, Abdul Khalil HPS. Cellulosic/synthetic fibre reinforced polymer hybrid composites: a review. Carbohydr Polym 2011;86:1–18. https://doi.org/10.1016/j.carbpol.2011.04.043.
[8] Esau K. Anatomy of seed plants. New York: Wiley; 1977.
[9] Ageeva MV, Petrovská B, Kieft H, Sal'nikov VV, Snegireva AV, Dam JEG, et al. Intrusive growth of flax phloem fibers is of intercalary type. Planta 2005;222:565–74. https://doi.org/10.1007/s00425-005-1536-2.
[10] Anderson DB. A microchemical study of the structure and development of flax fibers. Am J Bot 1927;14:187–211.
[11] Van Dam JEG, Gorshkova TA. Encyclopedia of applied plant sciences. Encycl. Appl. Plant Sci. Elsevier; 2003. p. 87–96. https://doi.org/10.1016/B0-12-227050-9/00046-6.
[12] Menoux Y, Katz E, Eyssautier A, De Parcevaux S. Résistance à la verse du lin textile: influence du milieu et critères de verse proposés. Agronomie 1982;2:173–80.

[13] Catling D, Grayson J. Identification of vegetable fibres. London: Archetype; 1982.
[14] Le Duigou A, Réquilé S, Beaugrand J, Scarpa F, Castro M. Natural fibres actuators for smart bio-inspired hygromorph biocomposites. Smart Mater Struct 2017;26:125009https://doi.org/10.1088/1361-665X/aa9410.
[15] Placet V, Day A, Beaugrand J. The influence of unintended field retting on the physicochemical and mechanical properties of industrial hemp bast fibres. J Mater Sci 2017;52:5759–77. https://doi.org/10.1007/s10853-017-0811-5.
[16] Alix S, Philippe E, Morvan C, Baley C. Putative role of pectins in the tensiles properties of flax fibres: a comparison between linseed and flax fibres varieties. Wageningen, The Netherlands: Pectins and Pectinases; 2008.
[17] Marrot L, Lefeuvre A, Pontoire B, Bourmaud A, Baley C. Analysis of the hemp fiber mechanical properties and their scattering (Fedora 17). Ind Crops Prod 2013;51:317–27. https://doi.org/10.1016/j.indcrop.2013.09.026.
[18] Baley C, Le Duigou A, Bourmaud A, Davies P, Nardin M, Morvan C, et al. Reinforcement of polymers by flax fibers: role of interfaces. Bio-based compos. high-performance mater. CRC Press; 2014. p. 87–112. https://doi.org/10.1201/b17601-7.
[19] Tanguy M, Bourmaud A, Beaugrand J, Gaudry T, Baley C. Polypropylene reinforcement with flax or jute fiber; influence of microstructure and constituents properties on the performance of composite. Ind Crops Prod 2017;139:64–74.
[20] Kelly A, Tyson WR. Tensile properties of fibre reinforced metals: copper/tungsten and copper/molybdenum. J Mech Phys Solids 1965;13:329–50.
[21] Braam J, Sistrunk ML, Polisensky DH, Xu W, Purugganan MM, Antosiewicz DM, et al. Plant responses to environmental stress: regulation and functions of the ArabidopsisTCH genes. Planta 1997;203:35–41. https://doi.org/10.1007/pl00008113.
[22] Bourmaud A, Gibaud M, Baley C. Impact of the seeding rate on flax stem stability and the mechanical properties of elementary fibres. Ind Crops Prod 2016;80:17–25. https://doi.org/10.1016/j.indcrop.2015.10.053.
[23] Milthorpe FL. Fibre development of flax in relation to water supply and light intensity. Ann Bot 1945;9:31–53.
[24] Niklas KJ. Plant height and the properties of some herbaceous stems. Ann Bot 1995;75:133–42. https://doi.org/10.1006/anbo.1995.1004.
[25] Lefeuvre A, Bourmaud A, Morvan C, Baley C. Tensile properties of elementary fibres of flax and glass: analysis of reproducibility and scattering. Mater Lett 2014;130:289–91. https://doi.org/10.1016/j.matlet.2014.05.115.
[26] ISO 1183–3. Plastics - Methods for determining the density of non-cellular plastics, Part 3: gas pyknometer method. Int Organ Stand 1999.
[27] Beaugrand J, Nottez M, Konnerth J, Bourmaud A. Multi-scale analysis of the structure and mechanical performance of woody hemp core and the dependence on the sampling location. Ind Crops Prod 2014;60:193–204. https://doi.org/10.1016/j.indcrop.2014.06.019.
[28] Coroller G, Lefeuvre A, Le Duigou A, Bourmaud A, Ausias G, Gaudry T, et al. Effect of flax fibres individualisation on tensile failure of flax/epoxy unidirectional composite. Compos Part A Appl Sci Manuf 2013;51:62–70. https://doi.org/10.1016/j.compositesa.2013.03.018.
[29] Shah DU. Damage in biocomposites: stiffness evolution of aligned plant fibre composites during monotonic and cyclic fatigue loading. Compos Part A Appl Sci Manuf 2015;83:160–8. https://doi.org/10.1016/j.compositesa.2015.09.008.
[30] Sader J, Sanelli J, Adamson B, Monty J, Wei X, Crawford S, et al. Spring constant calibration of atomic force microscope cantilevers of arbitrary shape. Rev Sci Instrum 2012;83:103705.
[31] Arnould O, Arinero R. Towards a better understanding of wood cell wall characterisation with contact resonance atomic force microscopy. Compos Part A-Appl Sci 2015;74:69–76.
[32] Corradini C, Cavazza A, Bignardi C. High-performance anion-exchange chromatography coupled with pulsed electrochemical detection as a powerful tool to evaluate carbohydrates of food interest: principles and applications. Int J Carbohydr Chem 2012;2012:1–13. https://doi.org/10.1155/2012/487564.
[33] Mussig J. Industrial applications of natural fibres: Structure, properties and technical applications; 2010.
[34] Chernova TE, Gorshkova T. Biogenesis of plant fibers. Russ J Dev Biol 2007;38:221–32.
[35] Cappelletto P, Brizzi M, Mongardini F, Barberi B, Sannibale M, Nenci G, et al. Italy-grown hemp: yield, composition and cannabinoid content. Ind Crops Prod 2001;13:101–13. https://doi.org/10.1016/S0926-6690(00)00057-1.
[36] Bourmaud A, Morvan C, Bouali A, Placet V, Perré P, Baley C. Relationships between micro-fibrillar angle, mechanical properties and biochemical composition of flax fibers. Ind Crops Prod 2013;44:343–51. https://doi.org/10.1016/j.indcrop.2012.11.031.
[37] Bledzki AKK, Franciszczak P, Osman Z, Elbadawi M. Polypropylene biocomposites reinforced with softwood, abaca, jute, and kenaf fibers. Ind Crops Prod 2015;70:91–9. https://doi.org/10.1016/j.indcrop.2015.03.013.
[38] Kundu A, Sarkar D, Mandal NA, Sinha MK, Mahapatra BS. A secondary phloic (bast) fibre-shy (bfs) mutant of dark jute (Corchorus olitorius L.) develops lignified fibre cells but is defective in cambial activity. Plant Growth Regul 2012;67:45–55. https://doi.org/10.1007/s10725-012-9660-z.
[39] Rowell R, Stout H. Jute, kenaf. In: ML, editor. Handb. fibre Chem. third ed. CRC Press, Boca Raton; 2007, p. 405–52.
[40] Alix S, Goimard J, Morvan C, Baley C. Influence of pectin structure on mechanical properties of flax fibres: a comparison between a linseed-winter variety (Oliver) and a fibres-spring variety of flax (Hermès). Pectins and Pectinases; 2009. p. 87–96.
[41] Mikshina P, Chernova T, Chemikosova S, Ibragimova N, Mokshina N, Gorshkova T. Cellulosic fibres: role of matrix polysaccharides in structure and function. Cellul – Fundam Asp 2013:91–112.
[42] Liu M, Fernando D, Meyer AS, Madsen B, Daniel G, Thygesen A. Characterization and biological depectinization of hemp fibers originating from different stem sections. Ind Crops Prod 2015;76:880–91. https://doi.org/10.1016/j.indcrop.2015.07.046.
[43]] Leuwin M. Handbook of fiber chemistry. Boca Raton; 2007.
[44] Ehresmann M, Amiri A, Ulven C. The effect of different variables on in-plane radial permeability of natural fiber mats. J Reinf Plast Compos 2018;37:1191–201. https://doi.org/10.1177/0731684416646458.
[45] Baley C. Analysis of the flax fibres tensile behaviour and analysis of the tensile stiffness increase. Compos Part A Appl Sci Manuf 2002;33:939–48.
[46] Salbu L, Bauer-Brandl A, Tho I. Direct compression behavior of low- and high-methoxylated pectins. AAPS Pharm Sci Tech 2010;11:18–26. https://doi.org/10.1208/s12249-009-9349-4.
[47] Le Gall M, Davies P, Martin N, Baley C. Recommended flax fibre density values for composite property predictions. Ind Crops Prod 2018;114:52–8. https://doi.org/10.1016/j.indcrop.2018.01.065.
[48] Bourmaud A, Malvestio J, Lenoir N, Siniscalco D, Habrant A, King A, et al. Exploring the mechanical performance and in-planta architecture of secondary hemp fibres. Ind Crops Prod 2017;108:1–5. https://doi.org/10.1016/j.indcrop.2017.06.010.
[49] Martin N, Mouret N, Davies P, Baley C. Influence of the degree of retting of flax fibers on the tensile properties of single fibers and short fiber/polypropylene composites. Ind Crops Prod 2013;49:755–67. https://doi.org/10.1016/j.indcrop.2013.06.012.
[50] Graupner N, Fischer H, Ziegmann G, Müssig J. Improvement and analysis of fibre/matrix adhesion of regenerated cellulose fibre reinforced PP-, MAPP- and PLA-composites by the use of Eucalyptus globulus lignin. Compos Part B Eng 2014;66:117–25. https://doi.org/10.1016/j.compositesb.2014.05.002.
[51] Eder M, Arnould O, Dunlop JWC, Hornatowska J, Salmen L, Salmén L, et al. Experimental micromechanical characterisation of wood cell walls. Wood Sci Technol 2013;47:163–82. https://doi.org/10.1007/s00226-012-0515-6.
[52] Bourmaud A, Baley C. Rigidity analysis of polypropylene/vegetal fibre composites after recycling. Polym Degrad Stab 2009;94:297–305. https://doi.org/10.1016/j.polymdegradstab.2008.12.010.
[53] Eder M, Arnould O, Dunlop JWC, Hornatowska J, Salmen L. Experimental micro-mechanical characterisation of wood cell walls. Wood Sci Technol 2012.
[54] Tanguy M, Bourmaud A, Baley C. Plant cell walls to reinforce composite materials: relationship between nanoindentation and tensile modulus. Mater Lett 2016;167:161–4. https://doi.org/10.1016/j.matlet.2015.12.167.
[55] Méndez-Vilas A, González-Martín M, Nuevo M. Optical interference artifacts in contact atomic force microscopy images. Ultramicroscopy 2002;92:243–50.
[56] Bourmaud A, Le Duigou A, Gourier C, Baley C. Influence of processing temperature on mechanical performance of unidirectional polyamide 11-flax fibre composites. Ind Crops Prod 2016;84:151–65. https://doi.org/10.1016/j.indcrop.2016.02.007.
[57] Madsen B, Lilholt H, Thygesen A, Arnold E, Weager B, Joffe R. Aligned flax fibre/polylactate composites : a materials model system to show the potential of bio-composites in engineering applications. J Nanostructured Polym Nanocompos 2008;8:139–45.
[58] Shah D, Nag N, Clifford M. Why do we observe significant differences between measured and 'back-calculated' properties of natural fibres? Cellulose 2016;23:1481–90. https://doi.org/10.1007/s10570-016-0926-x.
[59] Baley C, Bourmaud A. Average tensile properties of French elementary flax fibers. Mater Lett 2014;122:159–61. https://doi.org/10.1016/j.matlet.2014.02.030.
[60] Shah DU, Schubel PJ, Licence P, Clifford MJ. Determining the minimum, critical and maximum fibre content for twisted yarn reinforced plant fibre composites. Compos Sci Technol 2012;72:1909–17. https://doi.org/10.1016/j.compscitech.2012.08.005.